Impact of pre-pulse current and delay time on 46.9 nm laser with larger inner diameter alumina capillary

Muhammad Usman Khan, Yongpeng Zhao (赵永蓬)*, Dongdi Zhao (赵东迪), Huaiyu Cui (崔怀愈), Ziyue Cao (曹子悦), Bo An (安 博), and Feifei Zhang (张飞飞)

National Key Laboratory of Tunable Laser Technology, Institute of Optoelectronics, Department of Electronics Science and Technology, Harbin Institute of Technology, Harbin 150080, China

**Corresponding author: zhaoyp3@hit.edu.cn*

Received April 20, 2020; accepted July 22, 2020; posted online September 23, 2020

In this Letter, we firstly, to the best of our knowledge, demonstrated the influence of pre-pulse current and delay time on the intensity of a discharge pumped Ne-like Ar soft X-ray laser operating at 46.9 nm by employing an alumina capillary having an inner diameter of 4.8 mm. Specifically, the delay time was changed from 8 to 520 μs in small intervals. The pre-discharge current was increased from 25 A to 250 A through small steps, while keeping the main discharge current constant. Usually, a small pre-discharge current is applied to an Ar-filled capillary to attain a plasma column having sufficient pre-ionization before the injection of the main current. The pre-discharge current of 140 A was declared the best current to obtain lasing with a 4.8 mm diameter capillary. The laser spots were captured at best time delays for the pre-discharge currents of 25, 45, 80, 140, and 250 A, which support the experimental results. We observed that by applying the pre-discharge current of 140 A, the laser spot exhibits small divergence, higher symmetry, and uniformity, which is clear evidence of strong amplification. The laser spot obtained at 140 A is cylindrically symmetric and has a better structure than those reported by all other groups in the literature. Hence, the laser spot indicates that the laser beam is highly focusable and beneficial for the applications of the 46.9 nm laser. Results of this Letter might open a new way to enhance applications of a 46.9 nm capillary discharge soft X-ray laser.

Keywords: Z-pinch; pre-discharge; kink instabilities; beam divergence.

doi: 10.3788/COL202018.111403.

The short wavelength soft X-ray lasers (SXRLs) are important because of their numerous applications in science and technology. In many applications of SXRL, sufficiently high output laser pulse energy is required. Therefore, there have been consistent prior efforts toward the improvement of laser beam divergence, laser pulse energy, and output intensity of SXRL to expand their applications. There has been significant progress in the development of SXRL due to its potential usage in the field of fast process and micro-scale. In 1994, the Rocca group firstly, to the best of our knowledge, demonstrated the lasing through Ne-like Ar operating at 46.9 nm by employing capillary discharge pumped setup[1]. In their experiment, they used a 120 mm long capillary having an inner diameter of 4 mm. The research on capillary discharge SXRL is very important due to its numerous applications, such as nanoscale molecular imaging[2], extreme ultraviolet lithography[3], optical coherence tomography[4], ablation of solid targets[5], formation of nanostructures[6], actinide trace analysis and nanoscale isotopic imaging[7], SXRL holography[8], response of fusion plasma-facing materials[9], breaking of DNA strands[10], extreme ultraviolet nanoscale printing[11], and dynamics of converging laser created plasmas[12]. Furthermore, the applications of SXRL can be further extended by increasing energy per pulse and intensity.

Many research groups used pre-pulse discharge current to enhance the intensity of SXRL[13–17]. The intensity of SXRL can be enhanced by utilizing an appropriate pre-pulse discharge current before the injection of the main discharge current. The pre-ionization of Ar gas filled in an alumina capillary is achieved by the pre-pulse discharge current, which results in a low ionized plasma column before the injection of the main discharge current pulse. The main discharge current passes through the low ionized plasma column instead of breaking the neutral Ar gas. This is responsible for reducing the kink instability of Ar plasma during the Z-pinch process. As a result of the Z-pinch process, a highly ionized hot and dense plasma column is formed having axial uniformity. The population inversion in this highly ionized and hot plasma column is achieved between $3p^1S_0$ and $3s^1P_1$ levels by collisional excitation of ground state Ne-like Ar ions. Existence of highly stable and uniform axial plasma is an essential criterion for amplification of soft X rays in the capillary discharge plasma column. Axial inhomogeneity is commonly produced due to the electric discharge of high power as a consequence of slow compression and non-uniform initial conditions. To overcome this problem of non-uniformity of the plasma column, preformed plasma is produced by utilizing a suitable pre-pulse current before the arrival of the main discharge current.

In the present work, we firstly, to the best of our knowledge, demonstrate the influence of pre-pulse current and delay time on a 46.9 nm laser utilizing a 4.8 mm inner diameter alumina capillary for the best Ar pressure and main current amplitude to broaden its applications. To the best of our knowledge, no other groups utilized

 © 2020 Chinese Optics Letters

a 4.8 mm inner diameter alumina capillary to investigate the effect of pre-pulse current and delay time on the intensity of the 46.9 nm laser. In previous work, we investigated the influence of the capillary inner diameter on the 46.9 nm laser intensity by increasing the capillary inner diameter from 3.2 to 4.8 mm, and the 4.8 mm inner diameter alumina capillary was observed as the best choice for lasing[18]. Moreover, we also investigated the influence of the main discharge current on the laser output and observed a significant enhancement in laser intensity and energy[19]. The laser intensity and pulse energy strongly depend upon pre-discharge current and delay time between the pre-discharge and main discharge current. Therefore, it was necessary to investigate the best parameters such as pre-discharge current, delay time, initial Ar filling pressure, and main discharge current, which are very important to obtain a 46.9 nm capillary discharge laser. High main current amplitude is necessary to pinch the preformed Ar plasma in order to increase the intensity of the 46.9 nm laser, which can cause severe ablation of capillary material, and the intensity of the laser will decrease. The strong amplified emission can be achieved easily by employing a 4.8 mm inner diameter alumina capillary channel filled with Ar gas.

Conversely, the amplification for the smaller diameter is quite difficult because the material ablated from the capillary wall absorbs energy, which makes the laser amplification difficult. To overcome the ablation of capillary material, the utilization of a larger inner diameter capillary is the best choice. Moreover, the alumina capillary with a larger inner diameter is beneficial because of the larger gain volume to obtain an intense 46.9 nm laser.

The objective of this work is to improve the intensity of the 46.9 nm laser by changing experimental conditions, such as pre-discharge current, main discharge current, delay time, and initial filling pressure of Ar for the newly employed larger diameter alumina capillary. We experimentally demonstrate that the delay time between the pre-pulse current and main pulse discharge current plays a major role in the enhancement of laser intensity. The preformed plasma parameters, such as axial uniformity, plasma density, electron temperature, and change with time delay, influence the Z-pinch phenomenon injection of the main discharge current. Furthermore, we demonstrate that when the pre-discharge current is low, the laser intensity can be increased by decreasing the delay time between the pre-discharge and main discharge current. For high pre-discharge currents, the reverse is true. This change in laser intensity is most significant for the delay time between 8 and 45 μs. This change is less significant above these time delays. Experimental results demonstrate that the laser intensity decreases monotonically as the delay time goes above 45 μs. This observed reduction in laser intensity is due to the change of initial Ar pressure, absorption of laser in the plasma plume, non-uniformity of pre-ionized plasma density, and reduction of pre-ionized plasma density during the pre-discharge current pulse. Therefore, to overcome the non-uniformity of pre-ionized plasma density, the application of best delay time and pre-discharge current is beneficial in order to enhance the intensity of the 46.9 nm laser. Herein, we investigated the best pre-discharge current, best delay time, best initial Ar filling pressure, and main discharge current for the newly employed 4.8 mm inner diameter alumina capillary. The maximum laser pulse energy was estimated as approximately 1.5 mJ at the main discharge current of 40 kA with the best pre-discharge current and delay time, which is higher than the pulse energy reported by other groups and beneficial for 46.9 nm laser applications. The results of this work may bring new possibilities to maximize the applications of capillary discharge SXRL.

The pre-pulse and main pulse currents were used to generate the 46.9 nm laser. The circuit diagram of the pre-pulse power supply used in the experiments is shown in Fig. 1, which mainly includes these three parts: pre-pulse charging power supply, pre-pulse storage circuit, and pre-pulse trigger circuit. First, the storage capacitor is charged to a preset voltage of 21 kV by using a pre-pulse charging power source. When the pre-master pulse delay system outputs a pre-pulse trigger signal, the trigger circuit outputs a high voltage to the ball gap switch so that the ball gap switch is turned on. The voltage across the capacitor is applied to both ends of the capillary and discharges the gas within the capillary. A pre-pulse current flows through the capillary and produces plasma inside the capillary before the arrival of the main discharge current. By changing the value of the current limiting resistor, the amplitude of the pre-pulse current can be changed. The pre-pulse current was increased from 25 to 250 A by changing current limiting resistor. Moreover, when pre-discharge is produced inside the capillary due to the pre-pulse current, the trigger is turned on, which triggers the delay time circuit for the main current pulse. After the preset delay time between pre-pulse and main pulse, the main pulse generator is triggered by a signal. Eventually, a high amplitude main current is injected through the preformed plasma column in the capillary. A 35 cm long alumina capillary having an inner diameter of 4.8 mm is used to conduct the experiments to achieve an intense 46.9 nm laser.

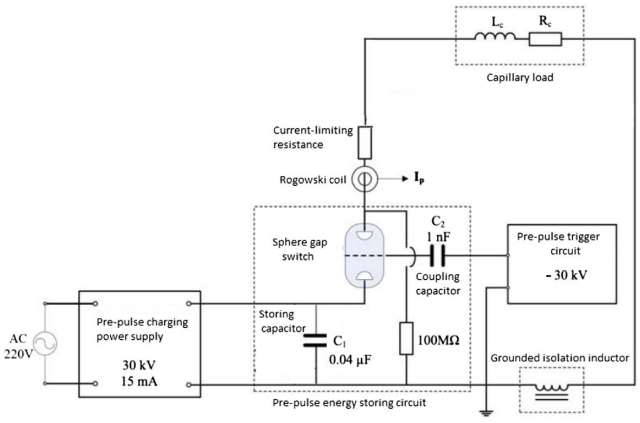

Fig. 1. Pre-pulse generating system.

The typical waveforms of the pre-current pulse are shown in Fig. 2. The main discharge current passes through the preformed plasma channel at time delays of several microseconds after the arrival of the pre-discharge current. A high amplitude main discharge current follows the exponentially decaying pre-pulse current. The pre-pulse current amplitude can be changed by the current limiting resistance of the discharge circuit. The synchronization between the pre-pulse current and main discharge current is measured by relative timings of the arrivals of current pulses of both pre-discharge and main discharge currents. It is interesting to find that the pre-discharge current amplitude decreases rapidly by increasing its amplitude. We increased the amplitude from 25 to 250 A and observed the change in pre-discharge current pulse time, and the pre-pulse time dropped significantly as we increased the pre-discharge current, up to 250 A. The pre-current pulse discharges the Ar-filled capillary. Consequently, the low-order pre-ionized plasma column having ions and free electrons is produced. After the preset delay time, the main discharge current flows through the preformed plasma column.

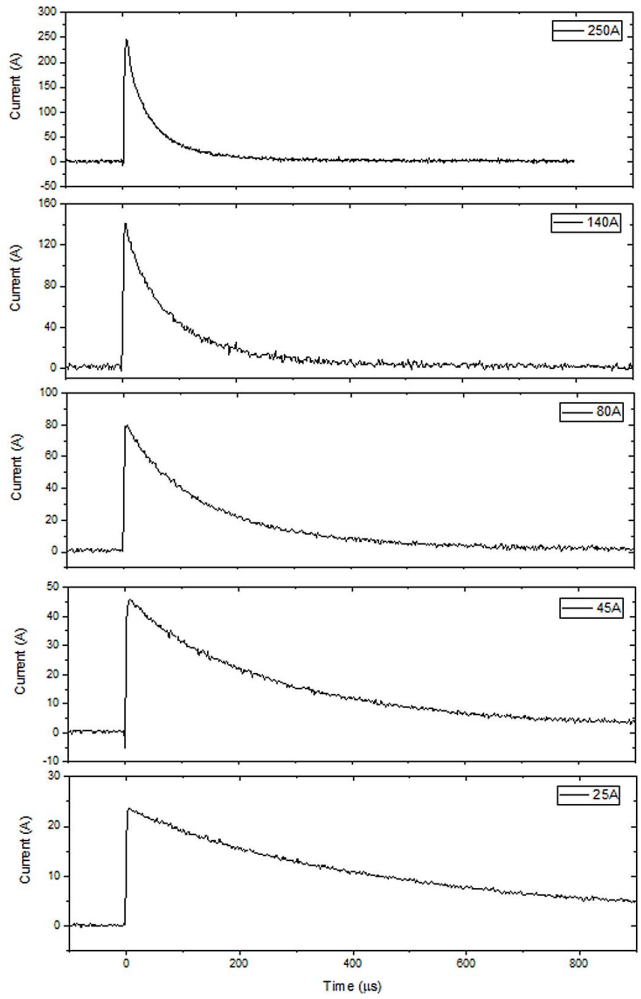

Fig. 2. Variation of 46.9 nm laser intensity as a function of delay time for different discharge currents.

The detailed description of the main pulse generator has been presented in Ref. [20]. A ten-stage Marx generator can produce an output voltage of approximately 300–450 kV. A water capacitor of 5 Ω, 3 nF is connected with the Marx generator. The water capacitor discharge through a self-breaking spark gap filled with N_2 into the Ar-filled alumina capillary results in the main discharge having the rise time about 35 ns and maximum amplitude in the domain of 30–45 kA. This high amplitude main discharge current produces a high-temperature Z-pinch plasma column in the 35 cm long alumina capillary having an inner diameter of 4.8 mm. According to requirements, the initial filling pressure of Ar gas inside the alumina capillary was used in the domain of 20–65 Pa by the continuous injection of Ar gas through a 4.8 mm axial hole in an electrode with the ground discharge electrode. The radiations emitted from the hole of the ground electrode transmit through a 2 mm pinhole fixed at a distance of 10 mm from the ground electrode. The distance between the ground electrode and pinhole must be small to reduce the absorption of the laser in Ar gas.

An X-ray diode (XRD) was utilized to measure background radiation and intensity of the 46.9 nm laser emitted by the highly dense and hot plasma column during the Z-pinch of Ar gas. The XRD contains a metal mesh anode and a gold-coated cathode, where the bias voltage of −600 V is applied to the gold-coated cathode to capture the temporal profile. An oscilloscope (Tektronix) having a bandwidth of 1 GHz was utilized to monitor and display the laser pulse coming from the XRD. The main discharge current of 30–40 kA was utilized to pinch the preformed Ar plasma achieved by pre-pulse current.

Figure 3 shows the dependence of 46.9 nm laser intensity on the delay time between pre-discharge and main discharge currents for five different pre-discharge currents of 25, 45, 80, 140, and 250 A. The experiments have been performed at an initial filling gas pressure of 43 Pa with a main discharge current of 30 kA. For each shot, the main discharge current, pre-pulse current, and delay time signals were measured by using a 1 GHz bandwidth oscilloscope. For all the pre-discharge currents shown, the laser intensity shows two characteristics as the pre-discharge current was increased: a relatively slow variation in laser intensity in the domain of 8 to 45 μs and a very sharp change in the regime of 45 to 520 μs. We increased the pre-discharge current from 25 to 250 A, whereas the delay time between the pre-pulse and main discharge currents was changed from 8 to 520 μs. For the pre-discharge currents (25–140 A), the laser intensity increases by increasing delay time up to 45 μs, but this trend is different in the delay time domain of 45 to 520 μs, where laser intensity decreases sharply. However, the observed characteristics of 140 A and 250 A pre-discharge currents are very similar, and much different from the rest of the cases. We investigated the optimum delay time and pre-discharge current by performing a series of experiments. The pre-discharge current of 140 A was observed as the best pre-discharge current for the larger inner diameter alumina capillary

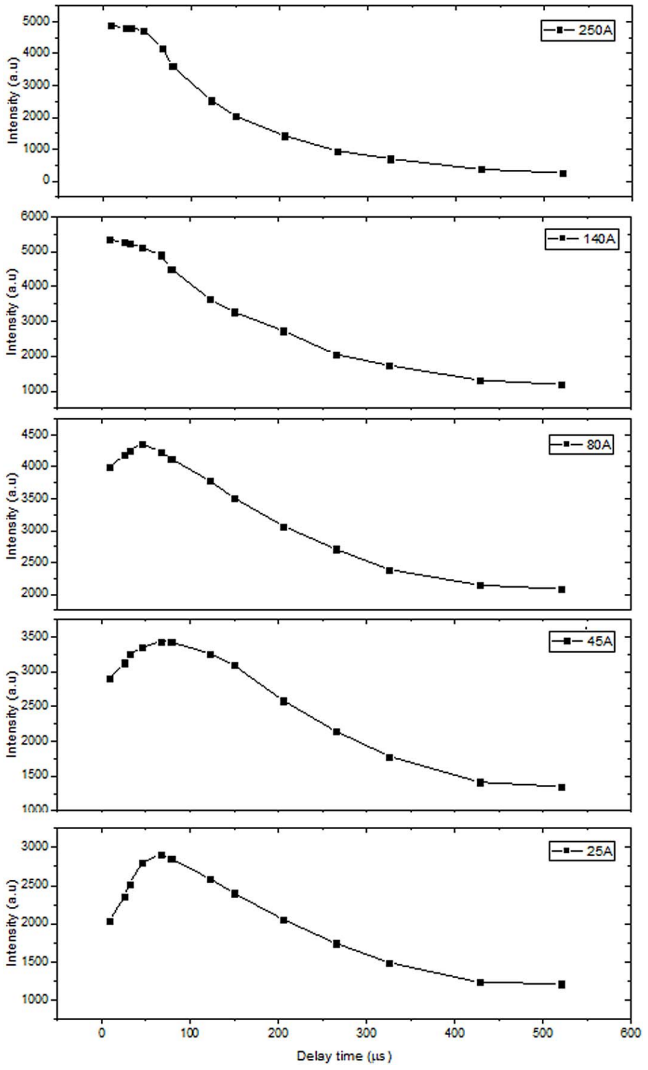

Fig. 3. Variation of 46.9 nm laser intensity as a function of delay time for different pre-discharge currents. The amplitude of the main discharge current was fixed at 30 kA.

having an inner diameter of 4.8 mm. The optimum value of delay time is within 40–100 μs and dependent on the pre-discharge current. Experimental results demonstrate that the optimum value of delay time is high for the low pre-discharge current. The delay time of 8 μs was observed as the best delay for the best pre-discharge current of 140 A. Therefore, apart from the pre-discharge current, the application of suitable delay time is also very important to prevent non-uniformity effects inside the preformed plasma before the onset of the main discharge current.

As the pre-discharge current passes through the capillary filled with Ar gas, it heats up Ar gas and generates sufficient pre-ionization. The increase of electron temperature and Ar pressure causes the ejection of the preformed plasma from the capillary opening. At the same time, sound waves in pre-ionized plasma are produced due to the axial flow of gas. The ejecting effect and sound waves bring individually a negative impact on the intensity of the laser. The axial non-uniformity is produced by the axial flow of sound waves, whereas the reduction of plasma density is caused by the ejecting effect[15,17]. The 2 mm pinhole at the capillary opening allows this pre-ionized gas to expand adiabatically, and this escape of pre-ionized Ar gas out of the capillary produces a relatively cold plasma plume, which expands adiabatically into the vacuum. This severely reduced the laser intensity for higher pre-discharge currents. If we suppose that the plasma is expanding in the vacuum, the plasma velocity can be calculated. The plasma plume velocity V can be estimated by using the expression[21,22]

$$V = \frac{2}{\gamma - 1} C_S. \tag{1}$$

The relationship between plasma parameters and ions acoustic velocity (C_S) of heated plasma is given by[23]

$$C_S = \sqrt{\frac{\gamma Z K_B T_e}{m_i}}. \tag{2}$$

Here, Z is the level of ionization, $\gamma = 5/3$ for Ar (monoatomic gases), T_e is electron temperature, K_B is Boltzmann constant, m_i is the mass of the single ion, and γ is the specific heat capacity. The plasma plume escape velocity can be calculated by combining Eqs. (1) and (2). It is clear from the above equations that the plasma plume velocity mainly depends upon the electron temperature. The electron temperature of the preformed plasma increases with the increasing amplitude of the pre-discharge current, which increases the escape velocity of plasma ejecting out from the capillary opening. The plasma plume ejecting out from the capillary opening passes through a 2 mm pinhole after traveling an approximately 10 mm distance from the capillary opening to the pinhole. The pinhole had a size of about 2 mm, which is much smaller than the capillary opening having a size of about 4.8 mm. Therefore, after passing out from the pinhole, its speed increases, which decreases the preformed plasma density significantly. At the same time, sound waves are produced due to the axial flow of gas. The sound waves and ejection of pre-ionized Ar gas bring a negative effect on the laser intensity. The axial flow of sound waves produces the axial non-uniformity, whereas the reduction of pre-ionized plasma is caused by the ejecting effect.

In the delay time domain of 8–50 μs, the amplitude of laser pulse increases and then decreases rapidly as the delay time goes above 45 μs for the pre-discharge currents of 25, 45 and 80 A, as shown in Fig. 3. This phenomenon can be explained by the fact that, for low discharge currents, the sound waves transmitted through a relatively short distance and reduction of pre-ionized plasma is negligible, whereas the laser intensity decreases sharply in the delay time range of 50–520 μs. Conversely, in the delay time of 8–50 μs, laser intensity decreases rapidly for pre-discharge currents of 140 and 250 A. In case of higher pre-discharge

currents, the effective length of the non-uniform pre-ionized plasma column caused by the axial flow of the sound wave is short. Meanwhile, the ejection of plasma density through the capillary opening is very high. Therefore, laser intensity decreases significantly due to the reduction of pre-ionized plasma density. Based on the above analysis, it is concluded that the influences from axial sound waves and the ejecting effect of pre-ionized plasma are negligible in the time delay range of 8–50 μs.

As shown in Fig. 3, the amplitude of the laser pulse decreases rapidly in the delay time domain of 50–520 μs. However, this reduction in laser intensity is higher for high pre-discharge currents. The reduction in laser intensity in this delay time regime is attributed to the increase of pre-ionized plasma density reduction and the non-uniform pre-ionized plasma length. This significant reduction in laser intensity for longer time delays indicates that pre-discharge currents continuously heat up the plasma. The speed of axial sound waves increases, which results in the non-uniformity of pre-ionized plasma before the injection of the main discharge current. As a result, laser intensity decreases severely in the delay time range of 50–520 μs. At the same time, the speed of plasma ejecting out from the capillary increases, leading to a significant reduction in pre-ionized plasma density, which severely decreases laser intensity. In conclusion, in the delay time domain of 50–520 μs, the drastic drop in laser intensity is due to non-uniformity caused by the axial flow of sound waves and reduction in pre-ionized plasma density as a result of the ejecting effect. According to Fig. 3, the optimum value of delay time is different for different pre-discharge currents. In case of low pre-discharge current, the optimum value of delay time is high. In case of high pre-discharge current, the optimum value of delay time is low. Therefore, for higher pre-discharge currents, sufficient pre-ionization can be obtained by applying a short time delay. The laser intensity decreases significantly by utilizing a pre-discharge current higher or lower than 140 A. Herein, a pre-discharge current of 140 A is declared the best prepulse current for lasing with the newly employed alumina capillary having an inner diameter of 4.8 mm, whereas 8 μs is declared as the best delay time to obtain sufficient pre-ionization.

In order to explore the region of best discharge parameters to obtain an intense and stable laser pulse, experiments were conducted at different conditions of the Ar initial filling pressure, main discharge current, and pre-discharge current. The dependence of laser intensity on the pre-pulse current is shown in Fig. 4. This experiment was performed by utilizing the main discharge current of 30 kA at the Ar filling pressure of 43 Pa. The alumina capillary having a length of 35 cm and inner diameter of 4.8 mm was utilized to produce uniformly ionized plasma columns. When the pre-pulse current is higher than 100 A, the laser pulse shows good reproducibility, whereas, for the pre-discharge current less than 100 A, the laser intensity decreases and results in less reproducibility.

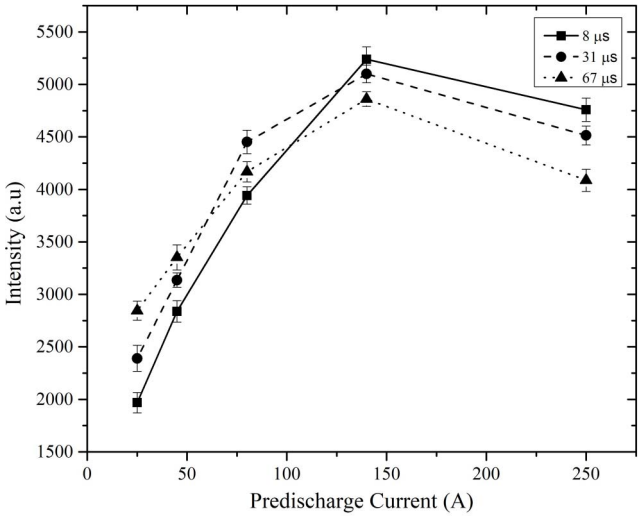

Fig. 4. Variation of laser intensity as a function of pre-pulse current.

The unstable laser pulse was observed for the low pre-discharge current, which was due to low pre-ionization. Moreover, the pre-discharge current of 140 A is observed as the best current to achieve lasing for three-time delays.

Initial investigations in Fig. 3 show that the amplitude of the laser is significantly high in the delay time range of 8 μs to 67 μs and drastically drops beyond 31 μs. The delay time below 31 μs shows significant sensitivity. The delay time below 67 μs was used in the detailed results described below. In order to study the dependence behavior of laser intensity on initial Ar filling pressure, two different time delays of 8 and 31 μs were used, while the pre-discharge current was kept constant. In this experiment, three different main currents of 30, 36, and 40 kA were used while keeping the pre-discharge current fixed at 140 A. Figure 5(a) illustrates the variation of the laser intensity with Ar pressure for the main current pulse of 30 kA. It is observed that the lasing pressure range is unaffected by delay time. The laser intensity for the delay time of 31 μs is lower in the pressure range below the optimum pressure. Conversely, when we increased the amplitude of the main current to 36 kA [Fig. 5(b)], the laser intensity in the pressure regime above the optimum pressure is higher in the case of 31 μs delay time. The intensity of the laser increased significantly as we increased the main discharge current from 30 to 40 kA. The optimum pressure for the main discharge current of 30, 36, and 40 kA is 43, 53, and 61 Pa, respectively. It is observed that with the increase of the main discharge current, the lasing pressure range becomes wider, and the laser intensity increases significantly.

The energy pre-pulse of the 46.9 nm laser was measured by a calibrated XRD and 1 GHz oscilloscope for main discharge currents of 30, 36, and 40 kA. The output laser intensity was reduced by employing stainless steel meshes of calibrated transmittivity to avoid XRD saturation. From the main discharge current of 20 to 40 kA, the laser energy

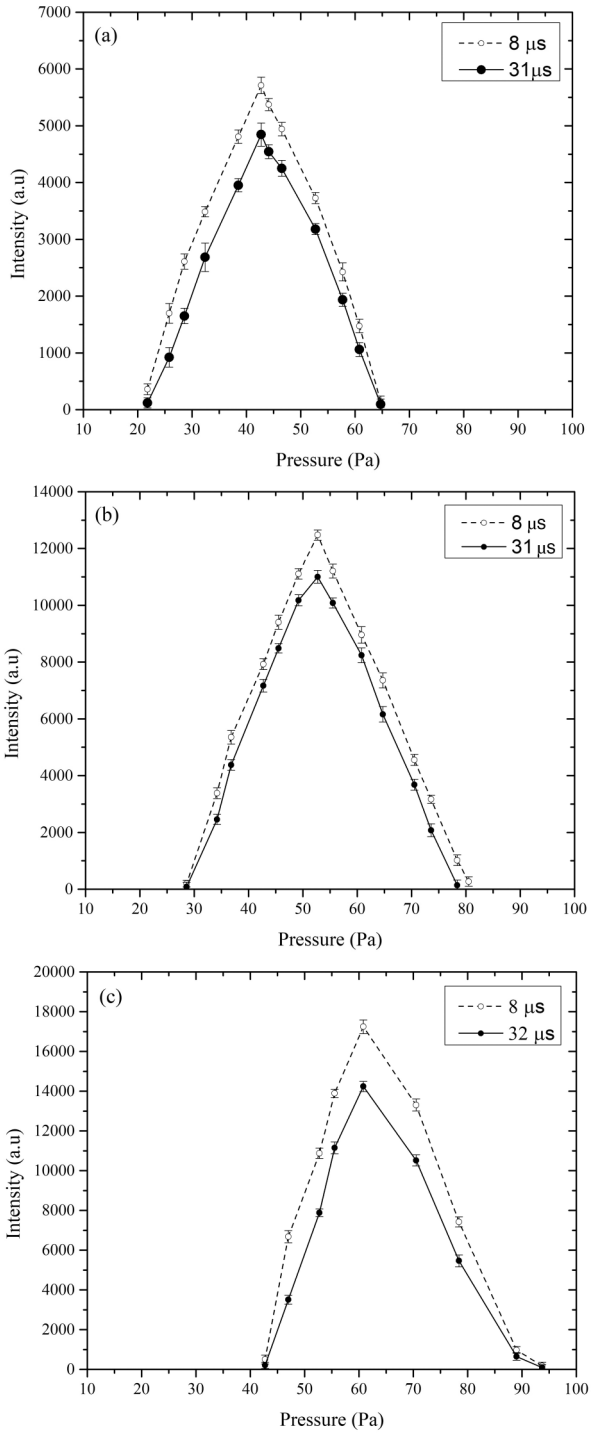

Fig. 5. Dependence of laser intensity on the initial filling pressure of Ar for two different delay times: (a) 30 kA, (b) 36 kA, and (c) 40 kA. The amplitude of pre-discharge current was set at 140 A throughout the experiment.

increased monotonically. When the main discharge current is 40 kA, the maximum laser pulse energy of 1.5 mJ is obtained at a discharge pressure of 60 Pa. The pre-discharge current was fixed at 140 A in this experiment. The Rocca group reported maximum laser pulse energy of 0.135 and 1 mJ by employing an alumina capillary with an inner diameter of 3.2 mm[24,25]. However, the maximum laser pulse energy reported in this work is much higher than previously reported results of pulse energy by other groups. It was observed that when the amplitude of the main discharge current increased, the value of the optimum laser pulse energy also increased. The results indicate that the utilization of this larger diameter capillary might enhance the applications of the 46.9 nm laser.

Figure 6 displays the estimated spatial intensity distribution of the laser beam having an annular shape. The knowledge of spatial intensity distribution and beam divergence of the 46.9 nm laser is of both basic and practical interest. In a capillary discharge device, the fast main discharge current pulse pinches the preformed plasma to produce a needle shape intense plasma column. The profile of the laser beam has an annular shape due to the refraction of amplified rays in the capillary channel due to a radial plasma density gradient inside the dense plasma column.

Because the X ray lies in the invisible region, the real images of laser spots were obtained by using a Ce-doped yttrium aluminum garnet (Ce:YAG) detector. To record laser spot images, the XRD was removed, and a sensitive X-ray detector was positioned inside a vacuum chamber in front of the laser at a distance of 170 cm from the exit of the capillary. The laser spots were captured with a Nikon camera of high-resolution at the best delay time for the pre-discharge currents of 25, 45, 80, 140, and 250 A, respectively. Image processing was performed to convert color images into grayscale images and to study intensity

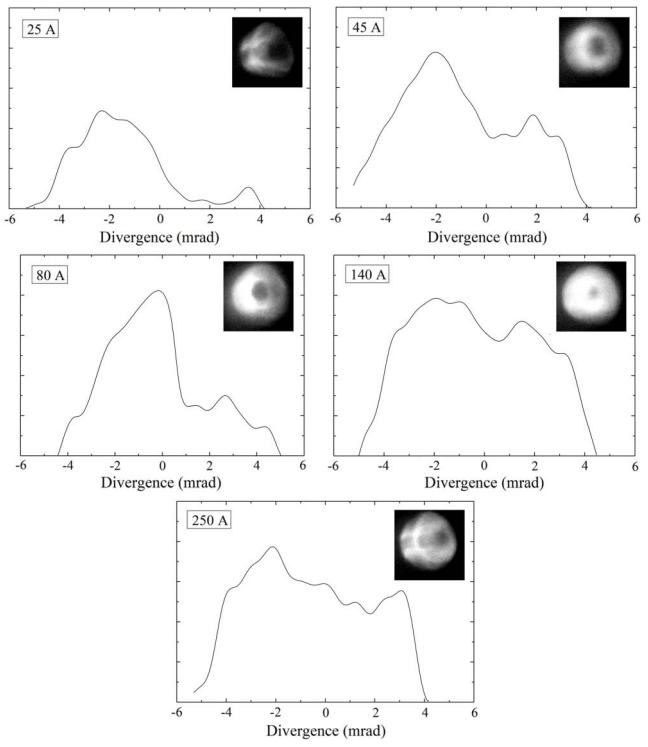

Fig. 6. Laser spots captured for different pre-discharge currents by utilizing a delay time of 8 μs. The main and pre-pulse currents were fixed at 30 kA and 140 A, respectively. The discharge pressure was set at 43 Pa for this experiment. The detection system is fixed at a distance of 170 cm from the capillary exit.

distribution and divergence of laser spots. Figure 6 clearly indicates that the output laser energy of the laser spot captured at 140 A appears to be more intense, symmetric, and uniform than in the spots captured at the 25, 45, 80, and 250 A pre-discharge current, which shows the best agreement with the analysis presented in Figs. 3 and 4. The laser spot captured at the 140 A pre-discharge current exhibits high symmetry, uniformity, and maximum laser pulse energy. Simultaneously, the intensity distribution of the laser beam changed from an annular shape to a single peak pattern with the pre-pulse current of 140 A. Therefore, the pre-pulse current of 140 A is declared as the best current to produce an intense 46.9 nm laser with newly employed larger diameter alumina capillary. The Rocca group investigated laser beam characteristics by using laser spots captured at different initial pressures[26,27]. However, our laser spots are cylindrically symmetric and have a better structure than those reported by all other groups for discharge pumped SXRL. The laser spot captured at the 140 A pre-discharge current indicates that the plasma is highly uniform, and the laser beam is highly focusable, which is beneficial for 46.9 nm laser applications. The measured value of peak to peak divergence is approximately 5 mrad. Moreover, the results obtained from laser spots are in accordance with the experimental results of laser intensity as a function of pre-discharge currents and time delays.

In conclusion, we firstly, to the best of our knowledge, demonstrate the influence of pre-pulse current and delay time on the energy per pulse and intensity of capillary discharge Ne-like Ar 46.9 nm laser with an alumina capillary having a 4.8 mm inner diameter. The influence of delay time was studied by increasing the delay time in the range of 8–520 μs. The spatial intensity distribution studies of laser spot shape have been performed by capturing a series of laser spots with the help of a high-resolution camera and Ce:YAG detector. The dependence of laser intensities on the pre-discharge current was studied in the the pre-discharge current range of 25–250 A. The maximum intensity of the 46.9 nm laser was observed for the pre-discharge current of 140 A. As can be expected, the pre-discharge current having a low amplitude (25 A) results in non-uniform heating of Ar gas during the pre-discharge current pulse, initiating kink instabilities in the plasma column during the Z-pinch produced by the high-amplitude main discharge current. The high-amplitude pre-discharge current (140 A) causes the stable collapse of the plasma column as a result of uniform heating of the gas. The pre-discharge current of 140 A is declared as the best current, whereas 8 μs is observed as the best delay time to achieve lasing in the 4.8 mm inner diameter alumina capillary. However, we found that for low discharge currents, the laser intensity can be increased by increasing delay time between the pre-discharge and main discharge currents. In addition, the laser intensity decreased significantly as we increased the pre-discharge current from 140 A to 250 A. We attributed this severe reduction in laser intensity to the ejecting effect, non-uniformity of preformed Ar plasma due to the flow of axial sound waves, absorption of the laser coming from the capillary by plasma plume, and change in initial Ar plasma density inside the capillary during the flow of pre-discharge current pulse. It is observed that while a certain pre-discharge current pulse is necessary for the operation of the 46.9 nm laser, the delay time for the main discharge current injection after the pre-pulse current is also very important to enhance energy per pulse and intensity of the laser. The maximum energy per pulse of 1.50 mJ was measured by employing a main current of 40 kA with the best pre-discharge conditions. The laser spot captured at 140 A is highly symmetric and has a better structure than those reported in the literature for a uniform capillary discharge laser. The results manifest that a pre-discharge current is a potential candidate to enhance laser pulse energy. The laser beam is highly focusable and favorable for applications of a 46.9 nm capillary discharge SXRL.

This work was supported by the National Natural Science Foundation of China (Nos. 61275139 and 61875045).

References

1. J. J. Rocca, V. Shlyaptsev, F. G. Tomasel, O. D. Cortazar, D. Hartshorn, and J. L. A. Chilla, Phys. Rev. Lett. **73**, 2192 (1994).
2. I. Kuznetsov, J. Filevich, F. Dong, M. Woolston, W. Chao, E. H. Anderson, E. R. Bernstein, D. C. Crick, J. J. Rocca, and C. S. Menoni, Nat. Commun. **6**, 7944 (2015).
3. M. C. Marconi and P. W. Wachulak, Prog. Quantum. Electron. **34**, 173 (2010).
4. P. Wachulak, A. Bartnik, and H. Fiedorowicz, Sci. Rep. **8**, 356 (2018).
5. Y. Zhao, H. Cui, W. Zhang, W. Li, S. Jiang, and L. Li, Opt. Express **23**, 14126 (2015).
6. Y. Zhao, H. Cui, S. Zhang, W. Zhang, and W. Li, Appl. Surface Sci. **396**, 1201 (2017).
7. T. Green, I. Kuznetsov, D. Willingham, B. E. Naes, G. C. Eiden, Z. Zhu, W. Chao, J. J. Rocca, C. S. Menoni, and A. M. Duffin, J. Anal. At. Spectrom. **32**, 1092 (2017).
8. P. W. Wachulak, M. C. Marconi, R. A. Bartels, C. S. Menoni, and J. J. Rocca, J. Opt. Soc. Am. B. **25**, 1811 (2008).
9. J. Straus, K. Kolacek, J. Schmidt, O. Frolov, M. Vilemova, J. Matejicek, A. Jager, L. Juha, Toutanova, A. Choukourov, and K. Kasuya, Laser Particle Beams **36**, 293 (2018).
10. E. Novakova, L. Vysin, T. Burian, L. Juha, M. Davidkova, V. Mucka, V. Cuba, M. E. Grisham, S. Heinbuch, and J. J. Rocca, Phys. Rev. E **91**, 042718 (2015).
11. L. Urbanski, A. Isoyan, A. Stein, J. J. Rocca, C. S. Menoni, and M. C. Marconi, Opt. Lett. **37**, 3633 (2012).
12. M. Purvis, J. Grava, J. Filevich, M. C. Marconi, J. Dunn, S. J. Moon, V. N. Shlyaptsev, E. Jankowska, and J. J. Rocca, Phys. Rev. E **76**, 046402 (2007).
13. A. Ben-kish, A. Ben-Kish, M. Shuker, R. A. Nemirovsky, A. Fisher, A. Ron, and J. L. Schwob, Phys. Rev. Lett. **87**, 015002 (2001).
14. Y. Hayashi, Y. Xiao, N. Sakamoto, H. Miyahara, G. Niimi, M. Watanabe, A. Okino, K. Horioka, and E. Hotta, Jpn. J. Appl. Phys. **42**, 5285 (2003).

15. M. Shuker, A. Ben-kish, R. A. Nemirovsky, A. Fisher, and A. Ron, Phys. Plasmas **13**, 013102 (2006).
16. G. Tomassetti, A. Ritucci, A. Reale, L. Palladino, L. Reale, S. V. Kukhlevsky, F. Flora, L. Mezi, J. Kaiser, A. Faenov, and T. Pikuz, Eur. Phys. J. D **19**, 73 (2002).
17. C. A. Tan and K. H. Kwek, Phys. Rev. A **75**, 043808 (2007).
18. H. Tong, Y. Zhao, M. U. Khan, Q. Yu, D. Zhao, F. Zhang, and Z. Cao, Eur. Phys. J. D **73**, 132 (2019).
19. M. U. Khan, Y. Zhao, T. Hui, M. K. Shahzad, H. Cui, and D. Zhao, Opt. Express **27**, 16738 (2019).
20. Y. Zhao, Y. Cheng, B. Luan, Y. Wu, and Q. Wang, J. Phys. D Appl. Phys. **39**, 342 (2006).
21. Y. P. Zhao, S. Jiang, Y. Xie, and Q. Wang, Appl. Phys. B **99**, 535 (2010).
22. Y. B. Zel'dovich and Y. P. Raizer, *Physics of Shock Waves and High-Temperature Hydrodynamic Phenomena* (Dover, 2002), p. 42.
23. J. D. Huba, *NRL Plasma Formulary* (The Office of Naval Research, 1998).
24. B. R. Benware, C. D. Macchietto, C. H. Moreno, and J. J. Rocca, Phys. Rev. Lett. **81**, 5804 (1998).
25. C. D. Macchietto, B. R. Benware, and J. J. Rocca, Opt. Lett. **24**, 1115 (1999).
26. C. H. Moreno, M. C. Marconi, V. N. Shlyapstev, B. R. Benware, C. D. Macchietto, J. L. A. Chilla, and J. J. Rocca, Phys. Rev. A **58**, 1509 (1998).
27. J. J. Gonzalez, M. Farati, J. J. Rocca, V. N. Shlyaptsev, and A. L. Osterheld, Phys. Rev. E **65**, 026404 (2002).